OpenFoam cases

Cavity

This is the classic lid-driven cavity benchmark: a square box with no-slip walls where the top wall moves at 1 m/s. The motion drives a recirculating vortex inside the cavity. The flow is treated as incompressible and laminar and solved with `icoFoam` on a uniform mesh (starting with a coarse grid).

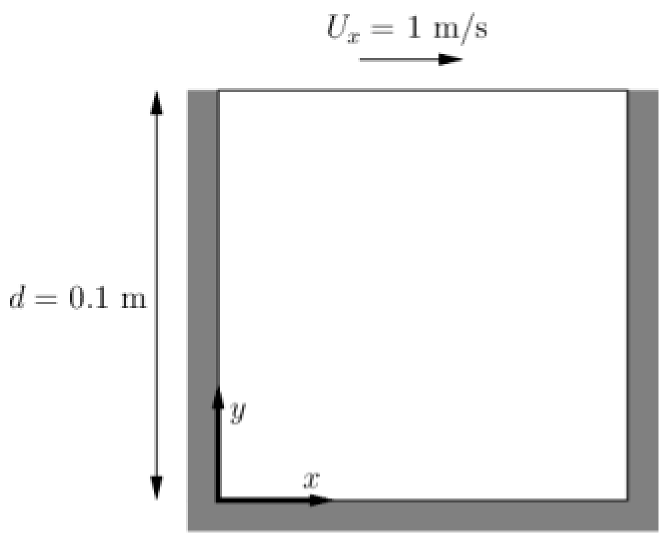

Figure 2.1: Geometry of the lid driven cavity.

Coarse mesh

We start with a coarse grid where we have 20 cells in both x- and y-direction and only one cell in the z-direction.

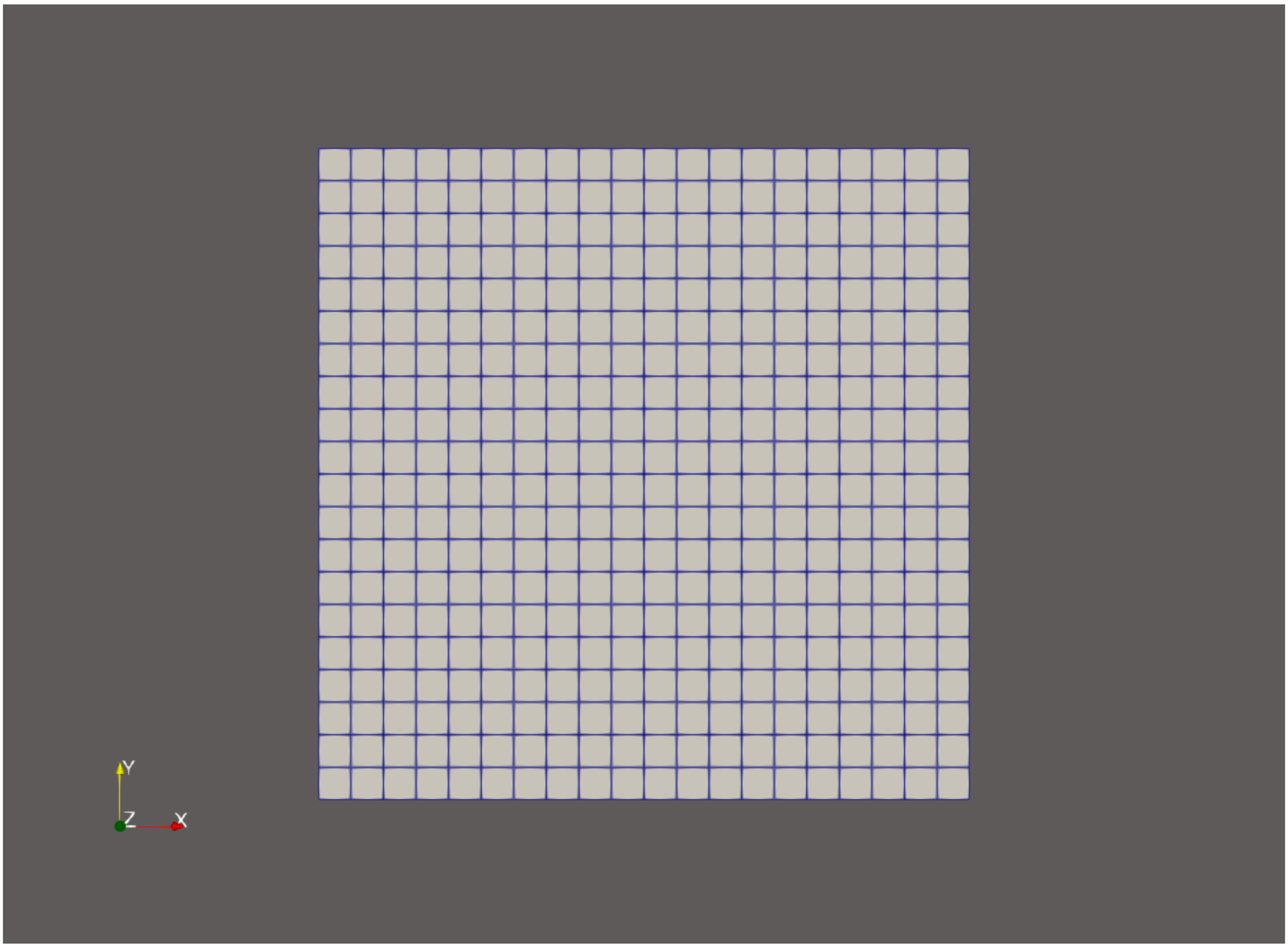

Velocity field

The velocity-vector plot (coloured by |U|) shows the moving lid creating a strong shear layer near the top wall and a primary recirculation vortex that fills most of the cavity.

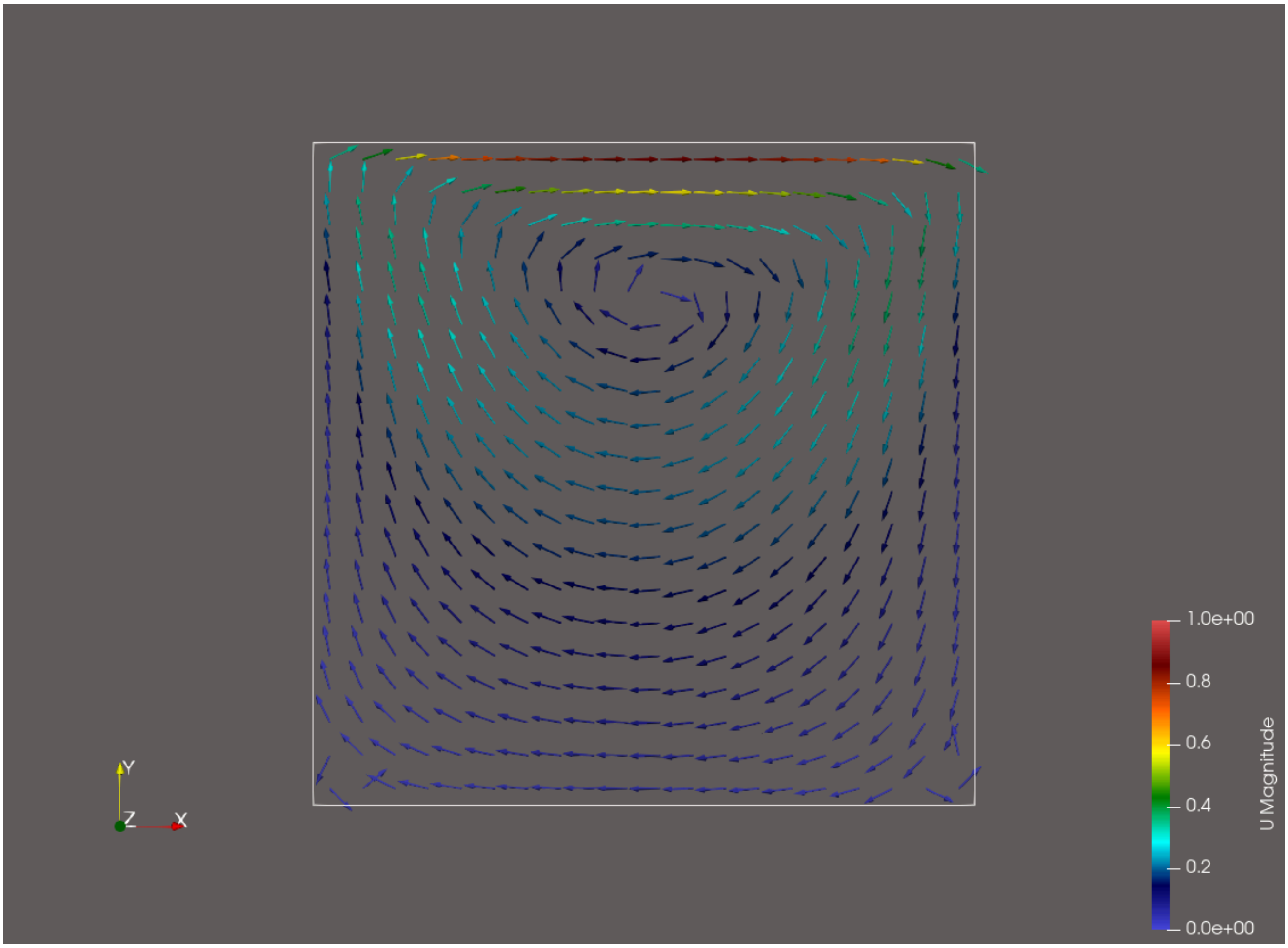

Streamfunction and streamlines

Streamlines make the main vortex structure easy to see: closed loops indicate recirculation. The streamfunction contour is another way to visualise the same motion—regions with tightly packed contours correspond to stronger velocity gradients (especially near the moving lid).

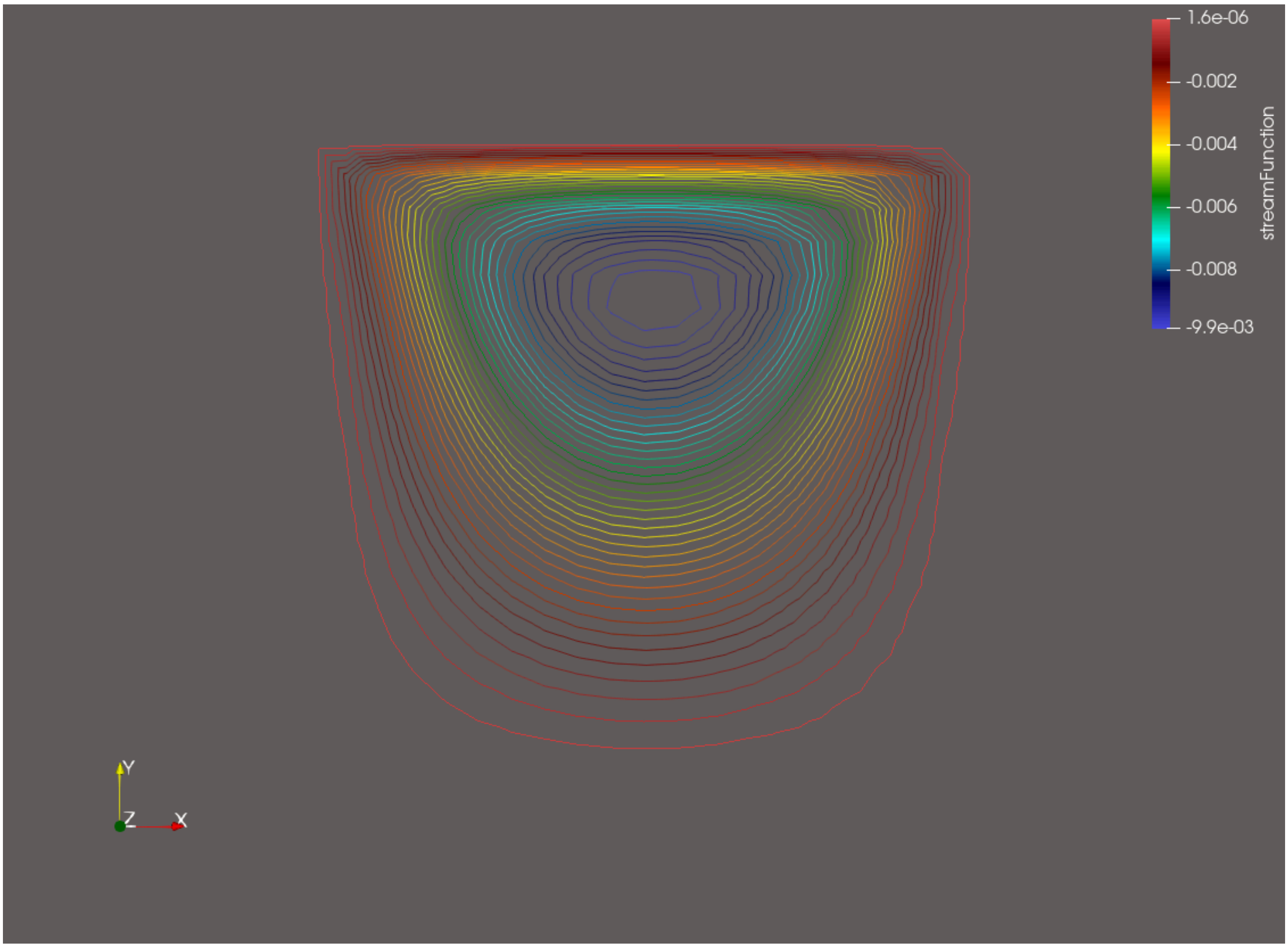

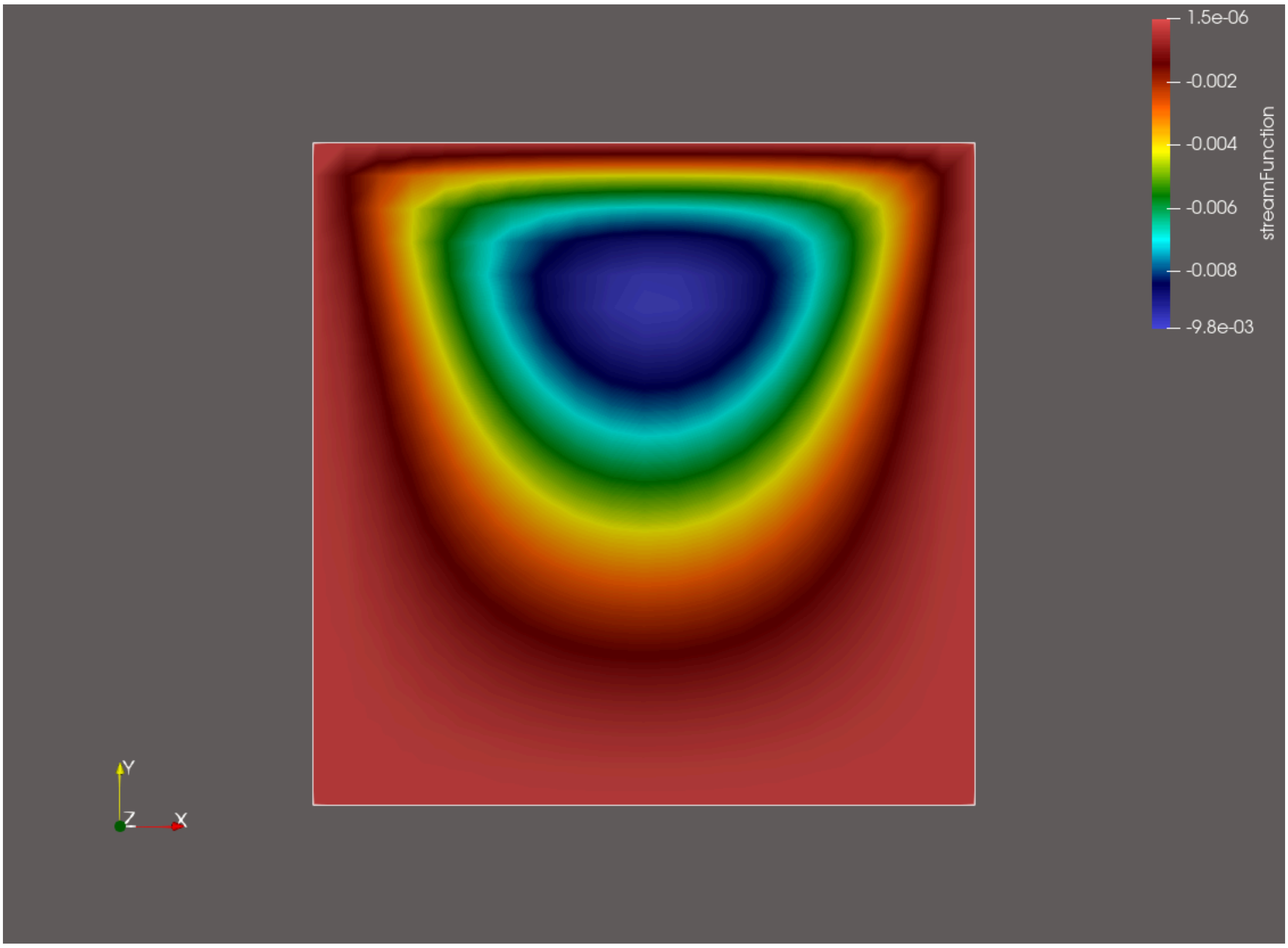

Pressure contours

The pressure contours(p/ρ) adjusts to support the turning/recirculating flow: higher and lower pressure regions form near the corners to balance the momentum changes.

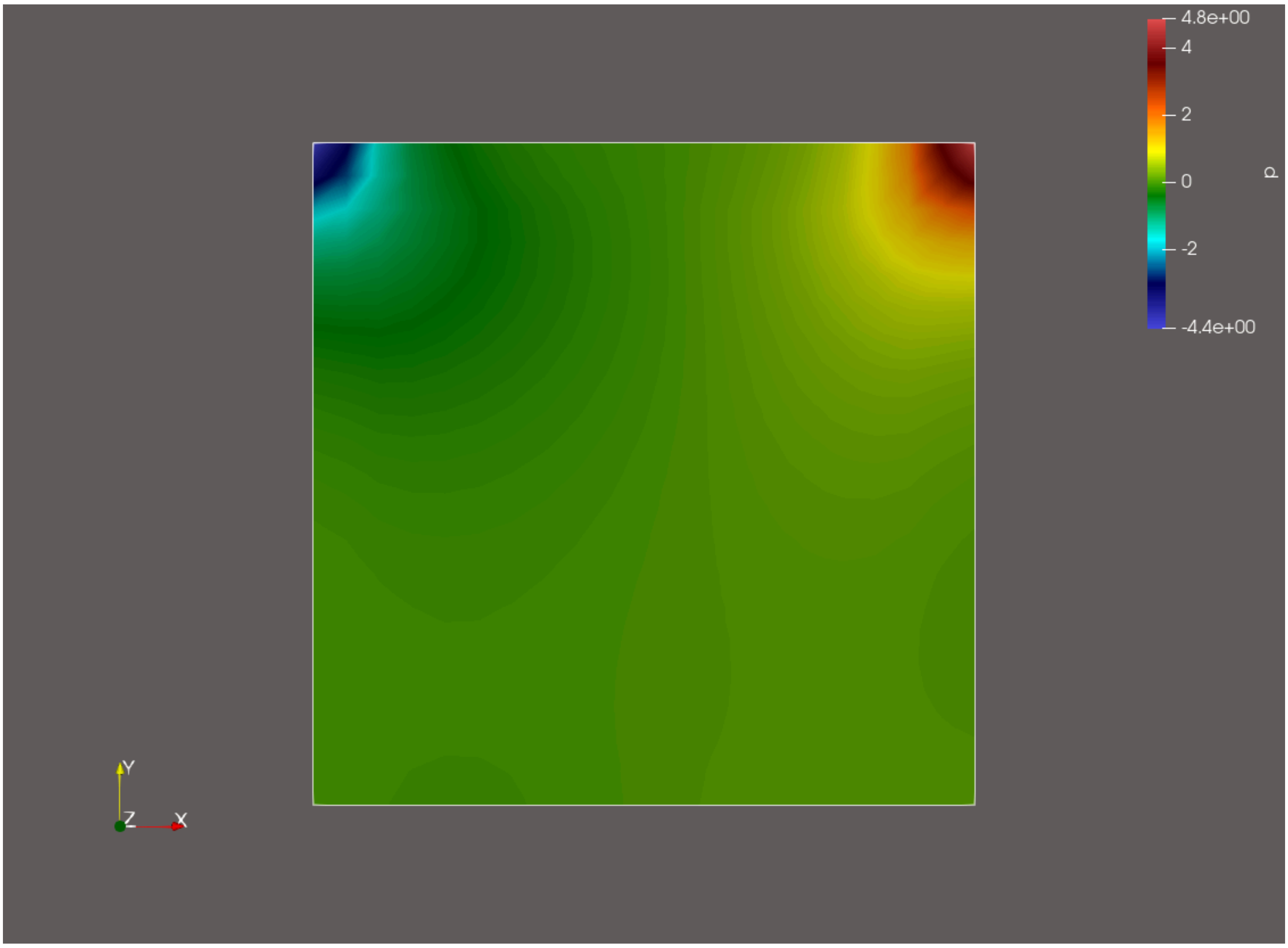

The centreline $U_x(y)$ profile shows reverse flow in part of the cavity (due to recirculation) and a rapid increase near the lid where the flow is driven forward.

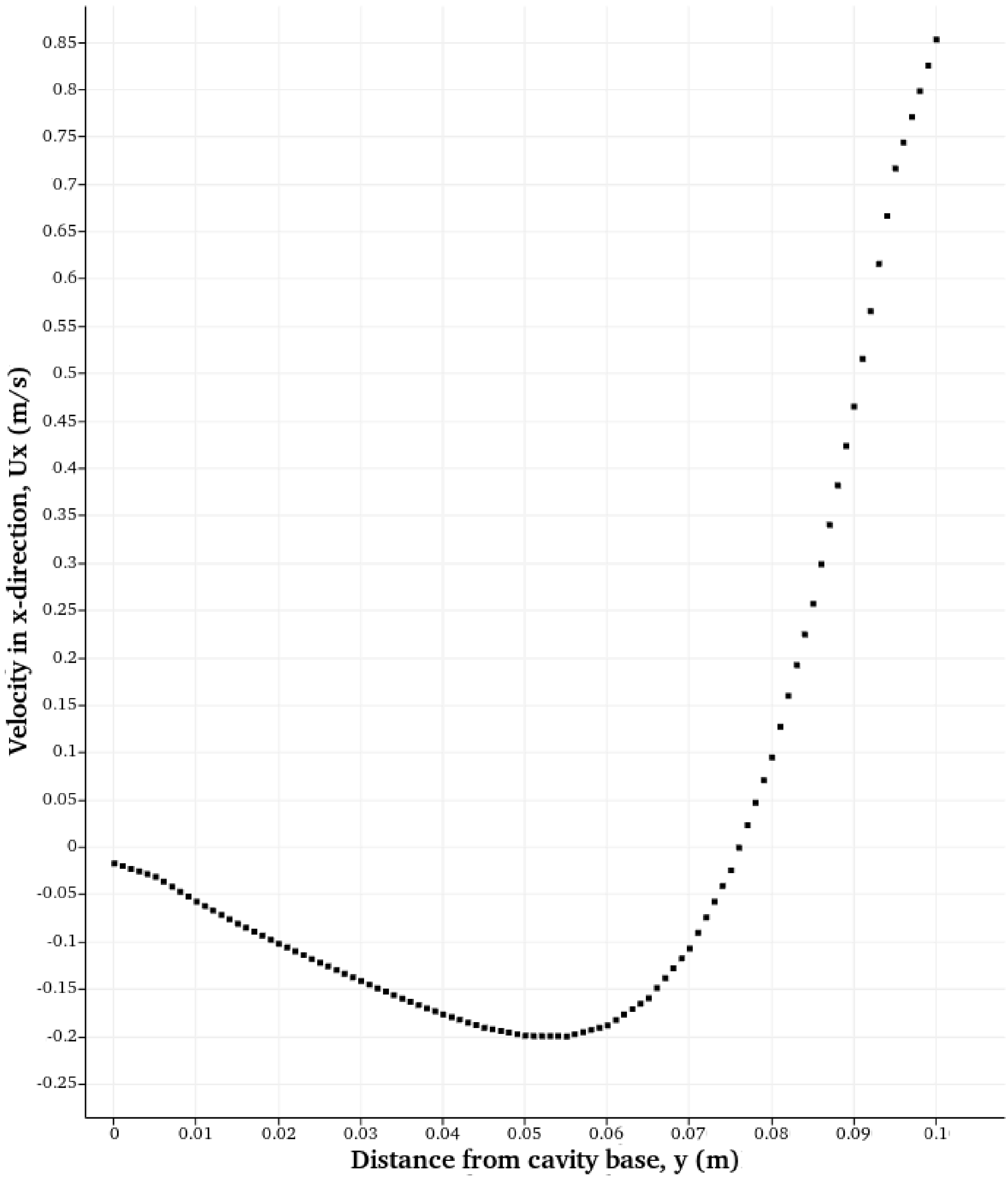

Fine mesh

Only the mesh is refined (from 20×20 to 40×40), which improves resolution of near-wall gradients and makes profiles smoother/more accurate. Using `mapFields` to initialise the fine mesh from the coarse steady solution reduces start-up transients and speeds up convergence.

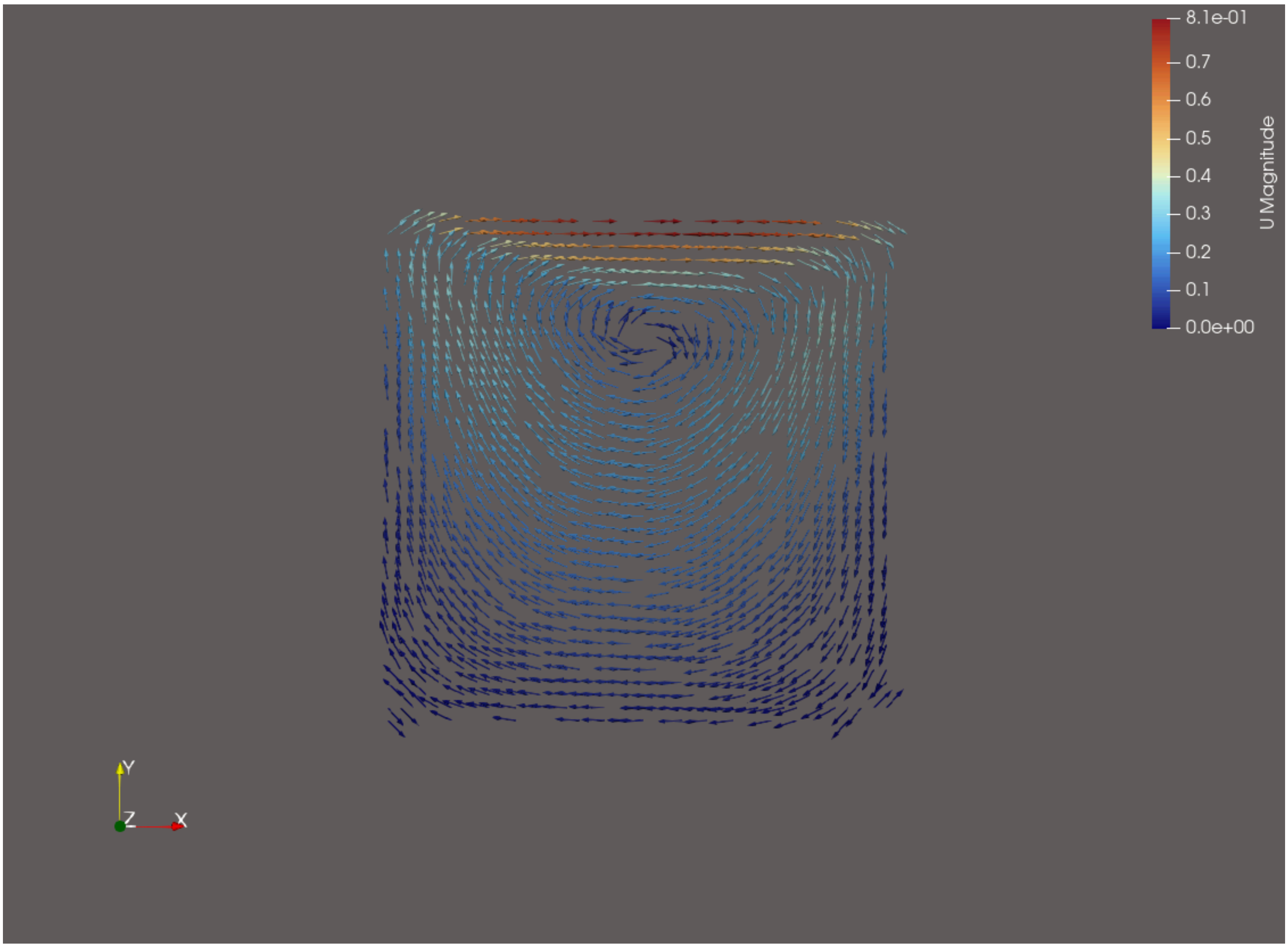

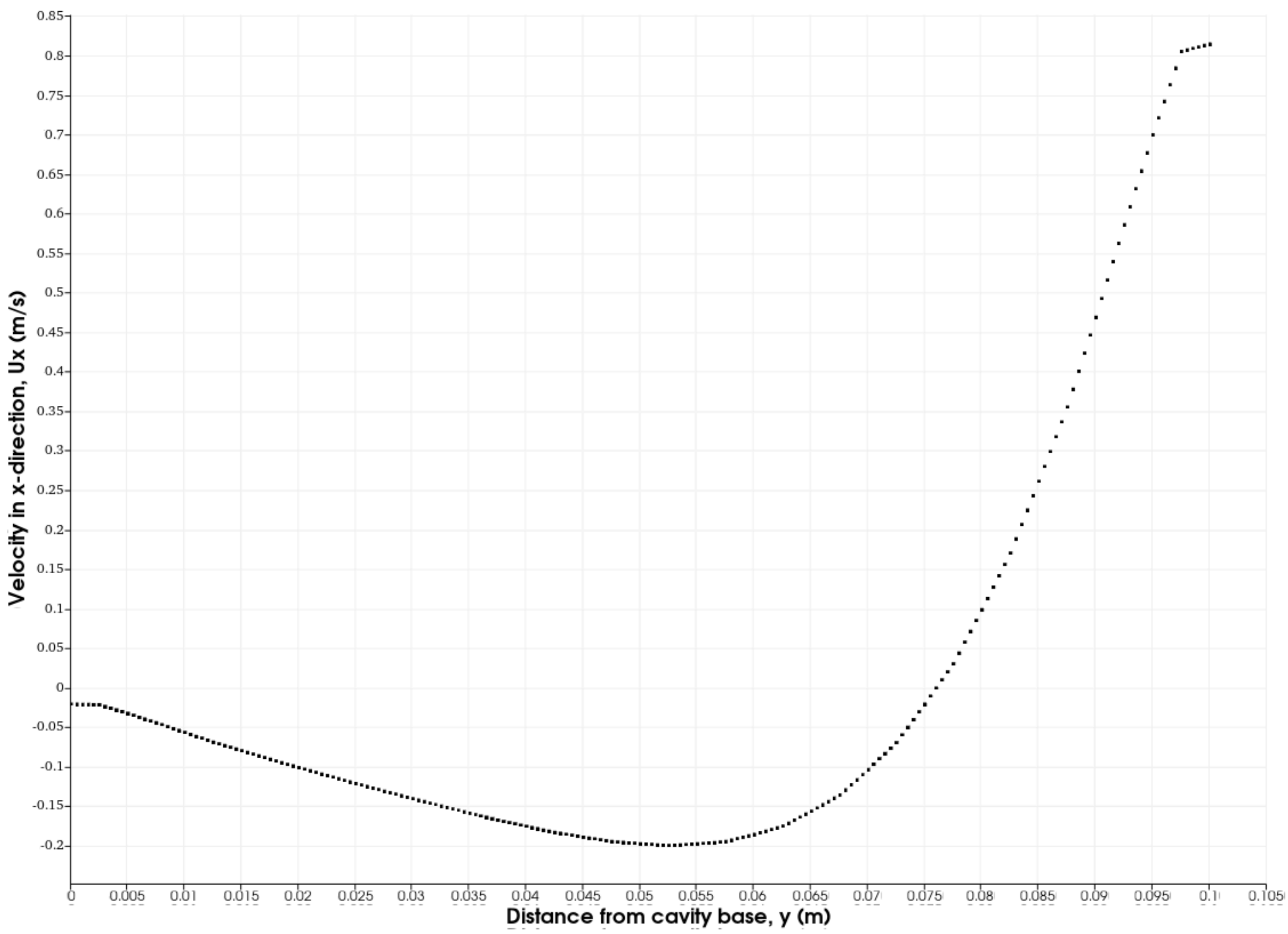

High Reynold

Here we increase the Reynolds number to 1000 and d = 1 m. At higher Reynolds number the flow becomes more “shear-layer dominated”: boundary layers get thinner and the vortex structure becomes more compact. The centreline velocity profile steepens near the lid, indicating stronger shear and more pronounced circulation effects. At $Re = 1000$ the velocity field shows sharper gradients and more complex flow features than the low-Re case

Velocity magnitude contours

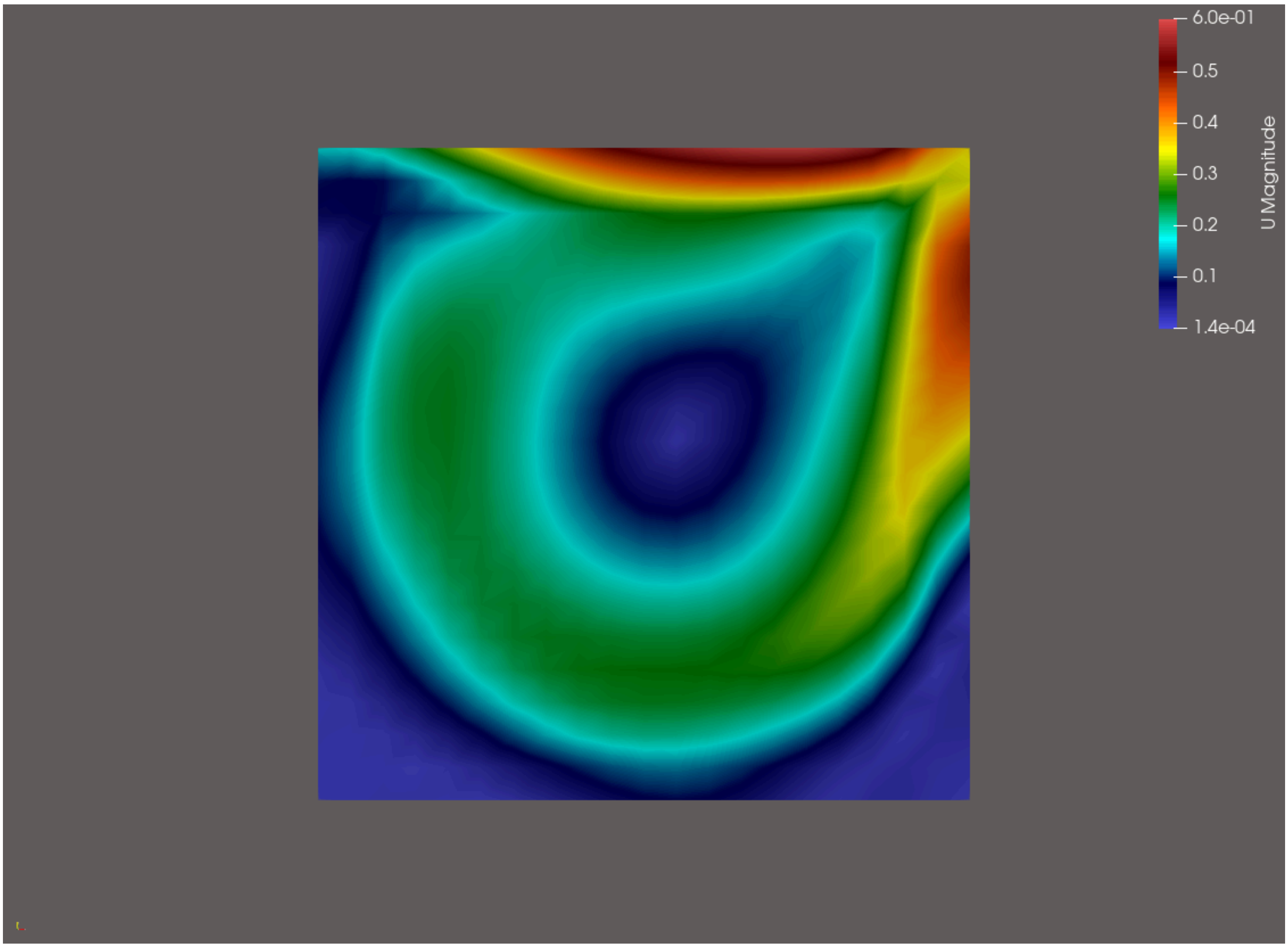

Vector field of the velocity

Vectors highlight the direction and strength of the circulating flow, while the streamfunction contours summarise circulation strength and vortex placement. Compared with lower Re, the vortex core location and secondary corner structures can change, reflecting stronger inertia and thinner boundary layers.

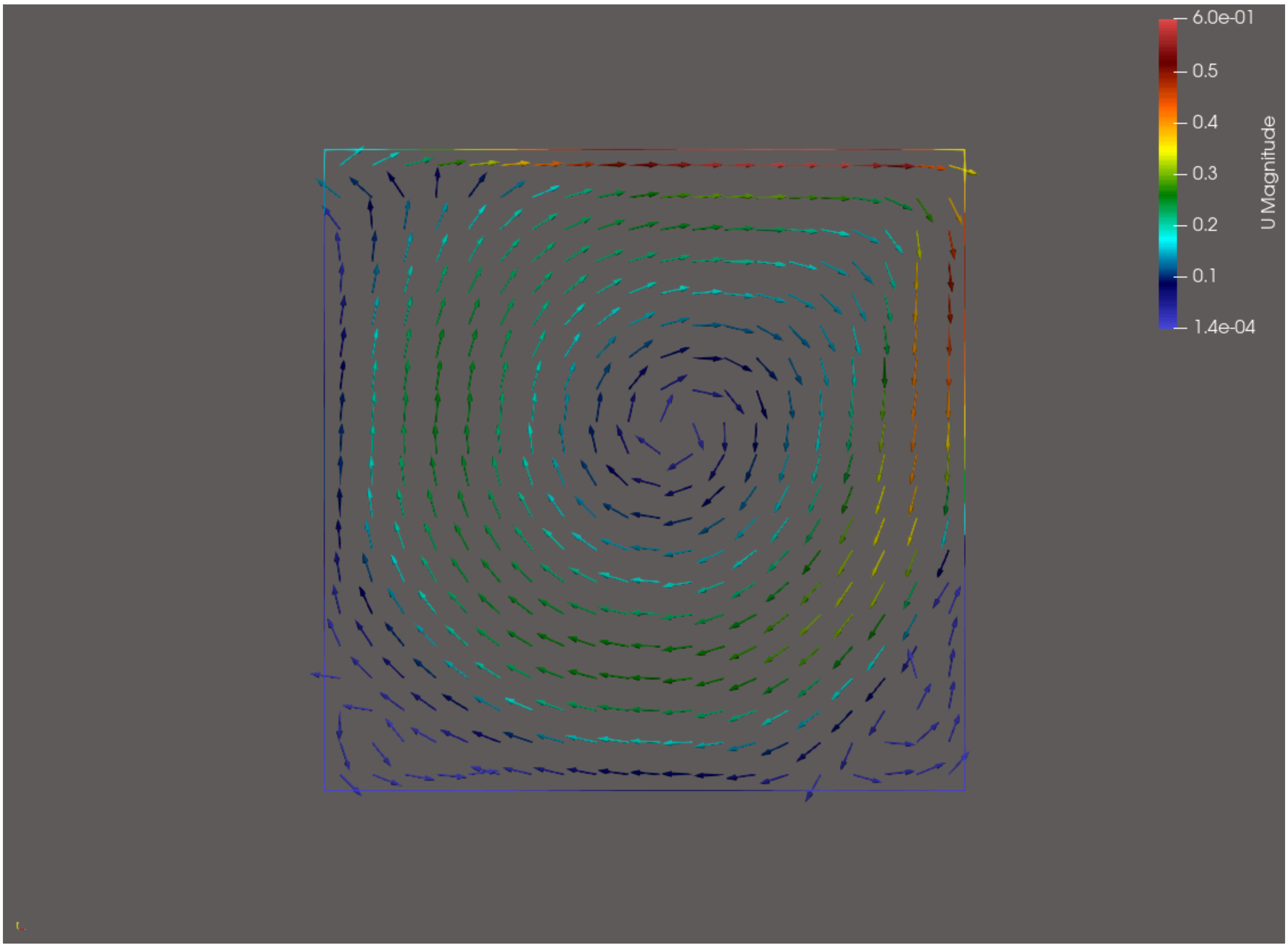

Streamfunction contours

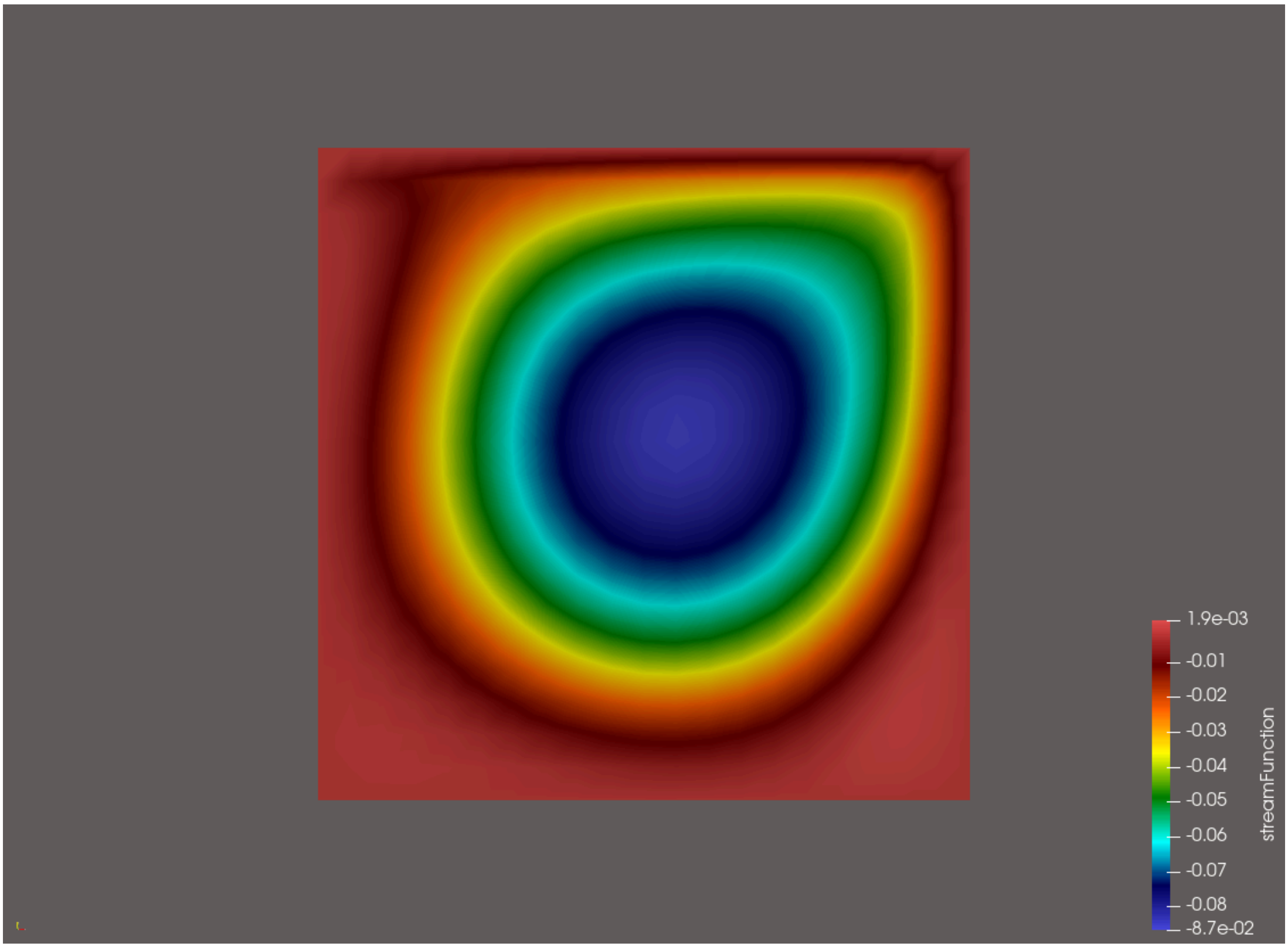

Streamlines

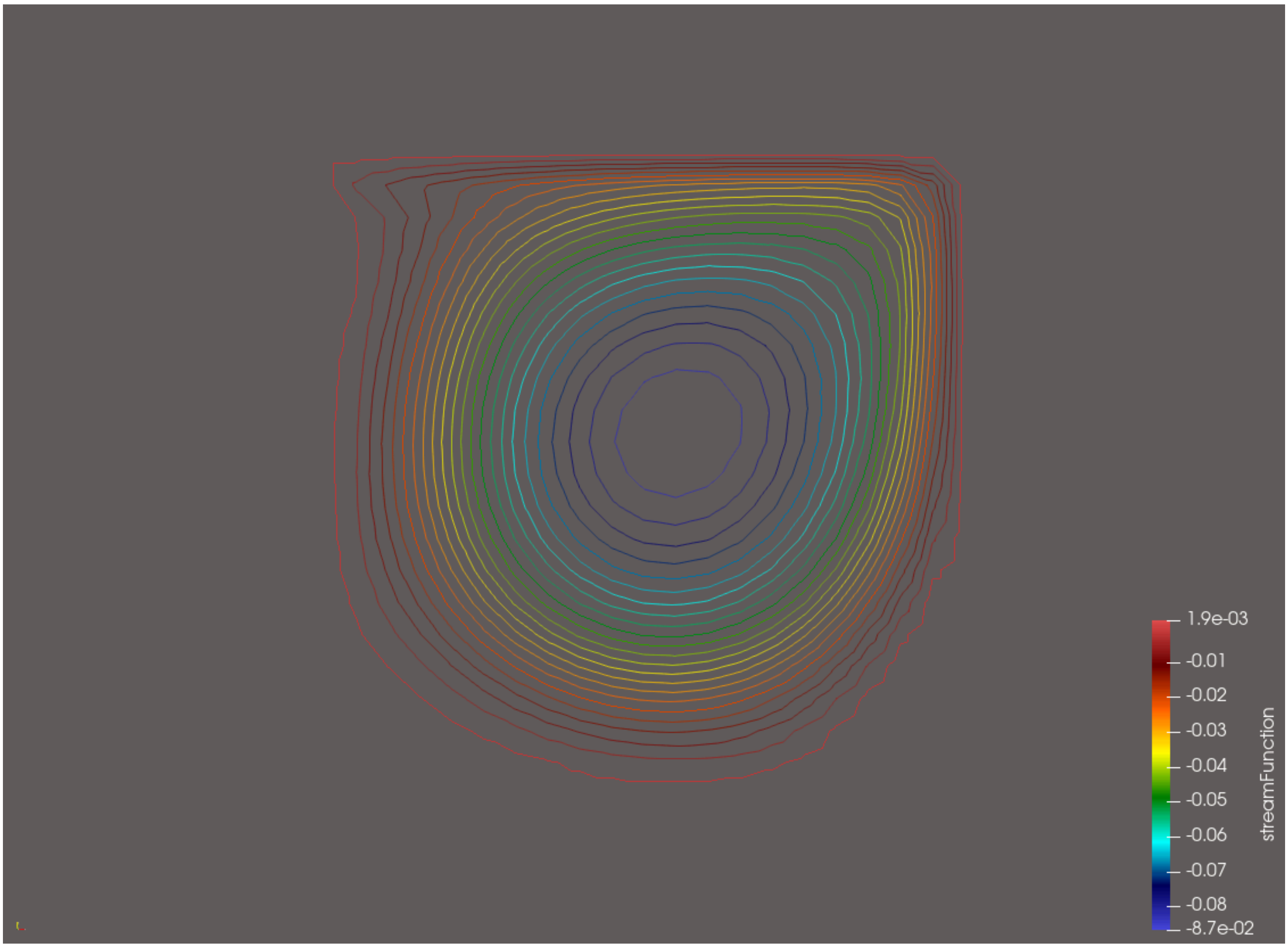

2D Air Foil

This is an incompressible, subsonic external flow over a 2D airfoil at angle of attack (α = 8°). Streamlines show acceleration over the suction side and a wake behind the trailing edge, which is where momentum deficit and losses appear.

Mesh

The mesh is refined around the airfoil to capture boundary-layer behaviour and the near-wake region. Finer cells near the leading and trailing edges help resolve strong gradients that influence lift and drag predictions.

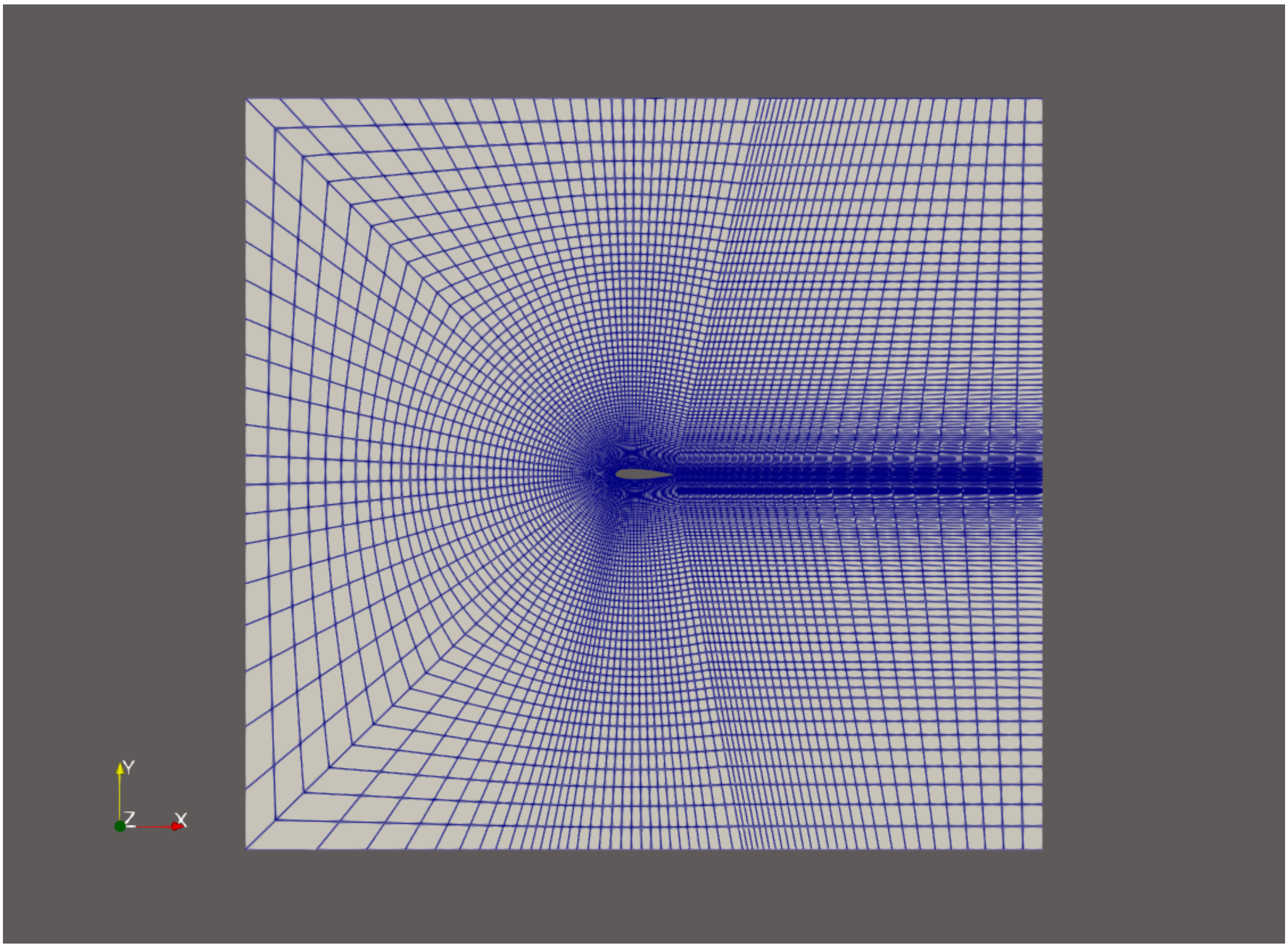

Velocity

The velocity magnitude contour shows higher speed over the suction side (typical for lift generation) and a velocity deficit in the wake. The wake thickness and the near-surface gradients are strongly affected by mesh resolution and solver convergence.

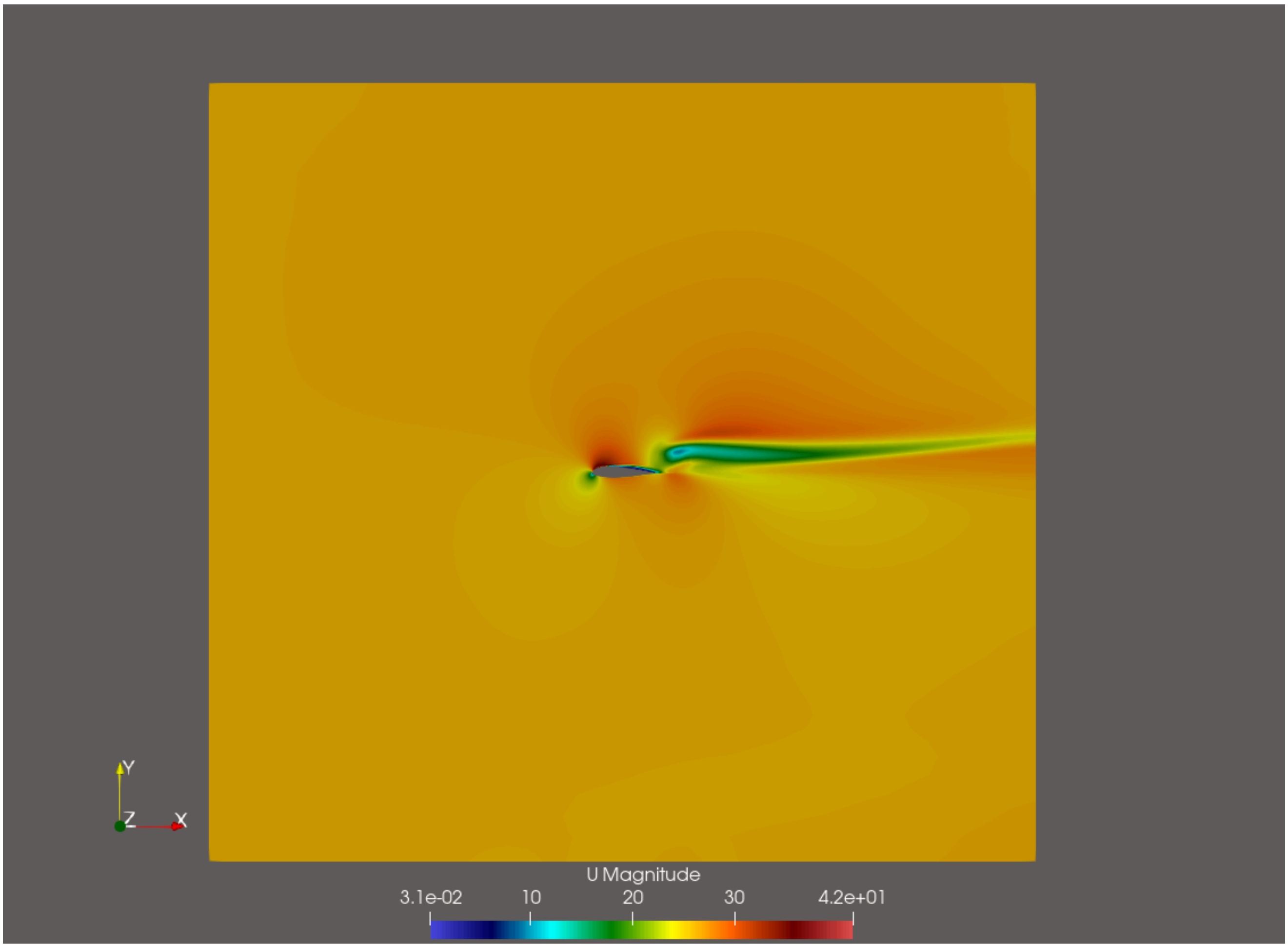

Pressure contours

This plot highlights where pressure is lower/higher around the airfoil. A lower-pressure region on the suction side and higher pressure on the pressure side are consistent with positive lift. Important to remember this is kinematic pressure (p/ρ).

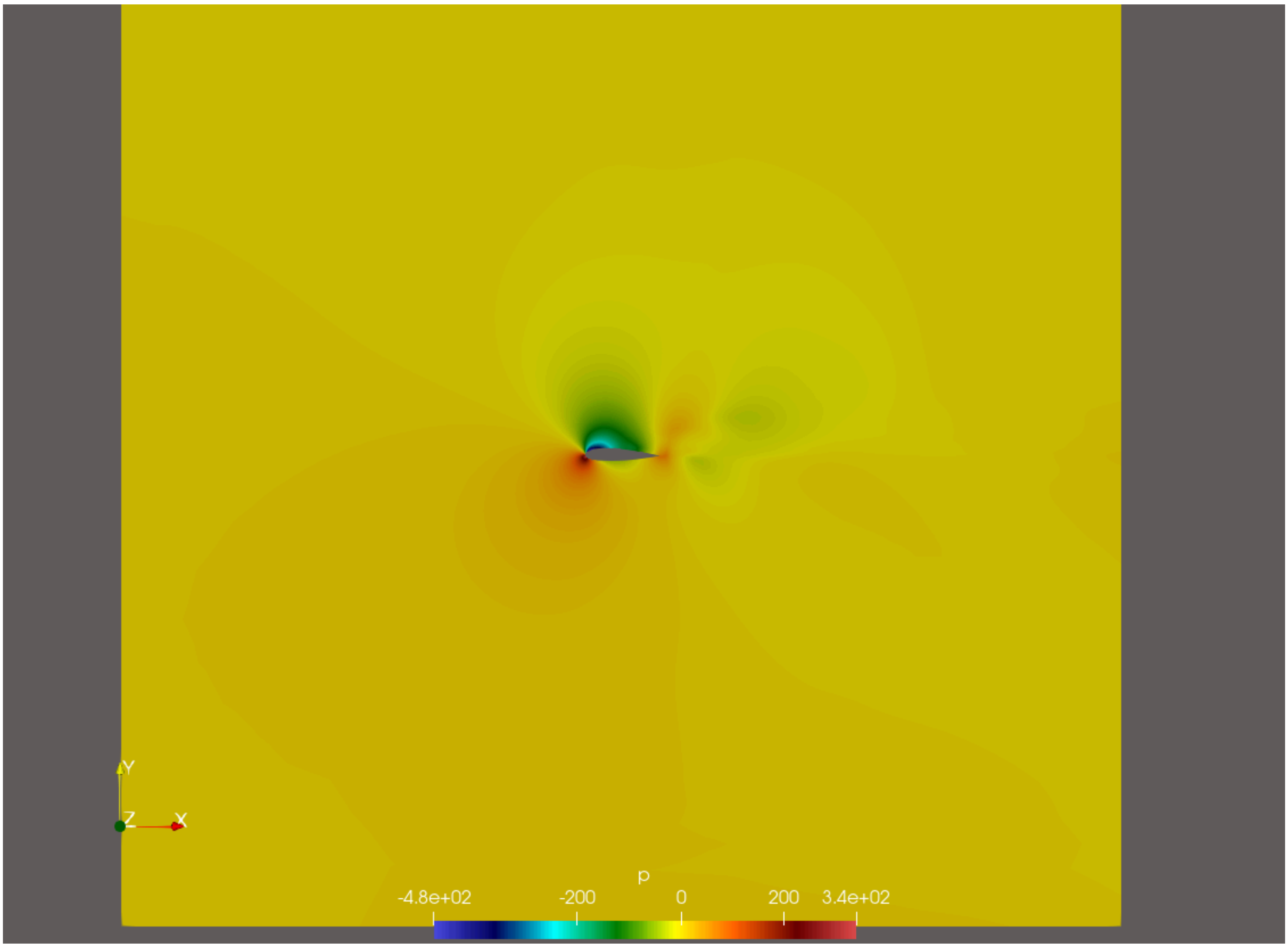

Lift and drag coeffs. vs iterations

The force coefficients (C_l, C_d) are tracked versus iteration to confirm the solution is converging to a steady state. The convergence plot shows how lift and drag settle after an initial transient/overshoot.

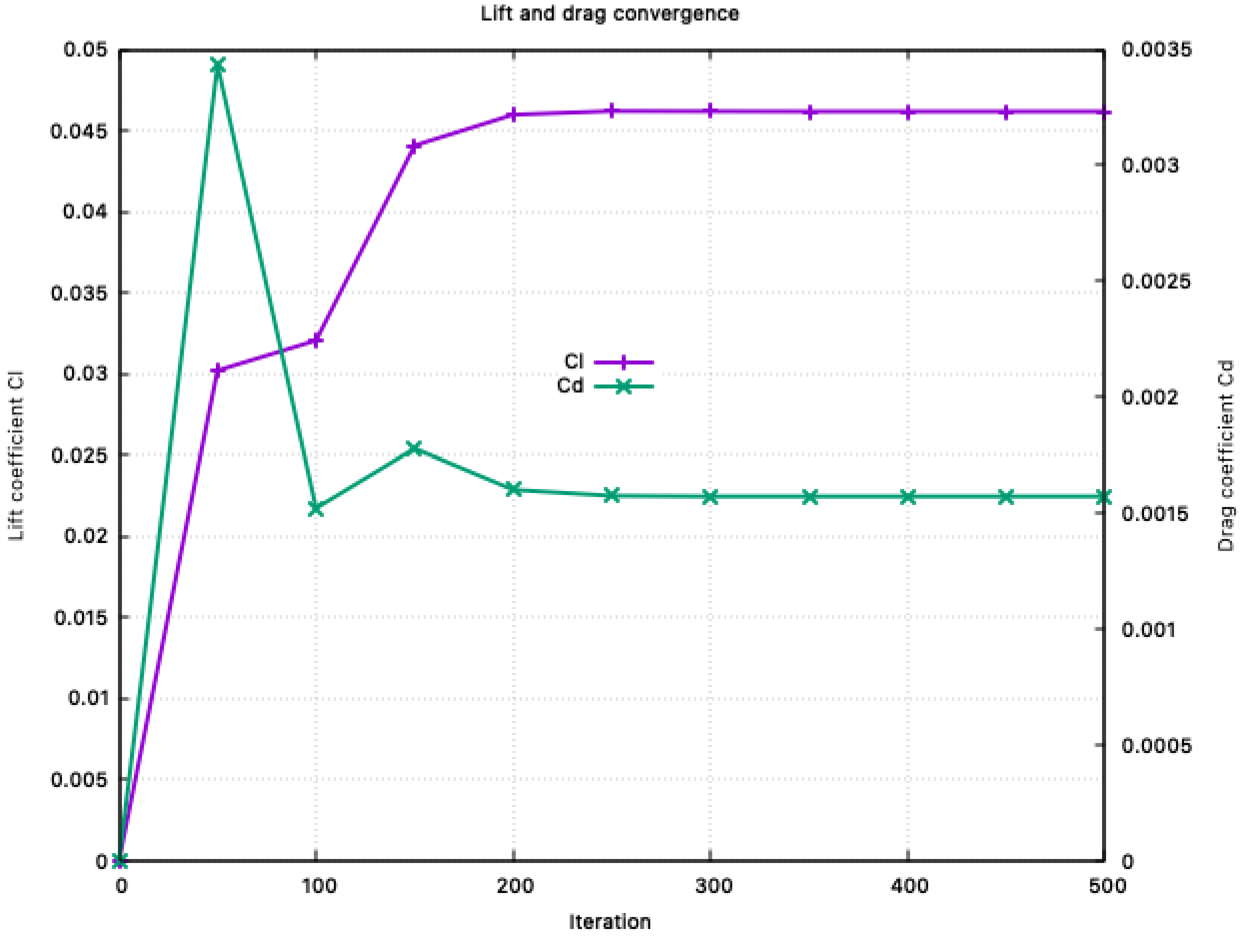

Drag decomposition vs iterations

The drag decomposition separates viscous (skin-friction) and pressure (form) contributions. Here we can see that both decompositions contribute the same until 100 iterations, then the pressure part takes over.

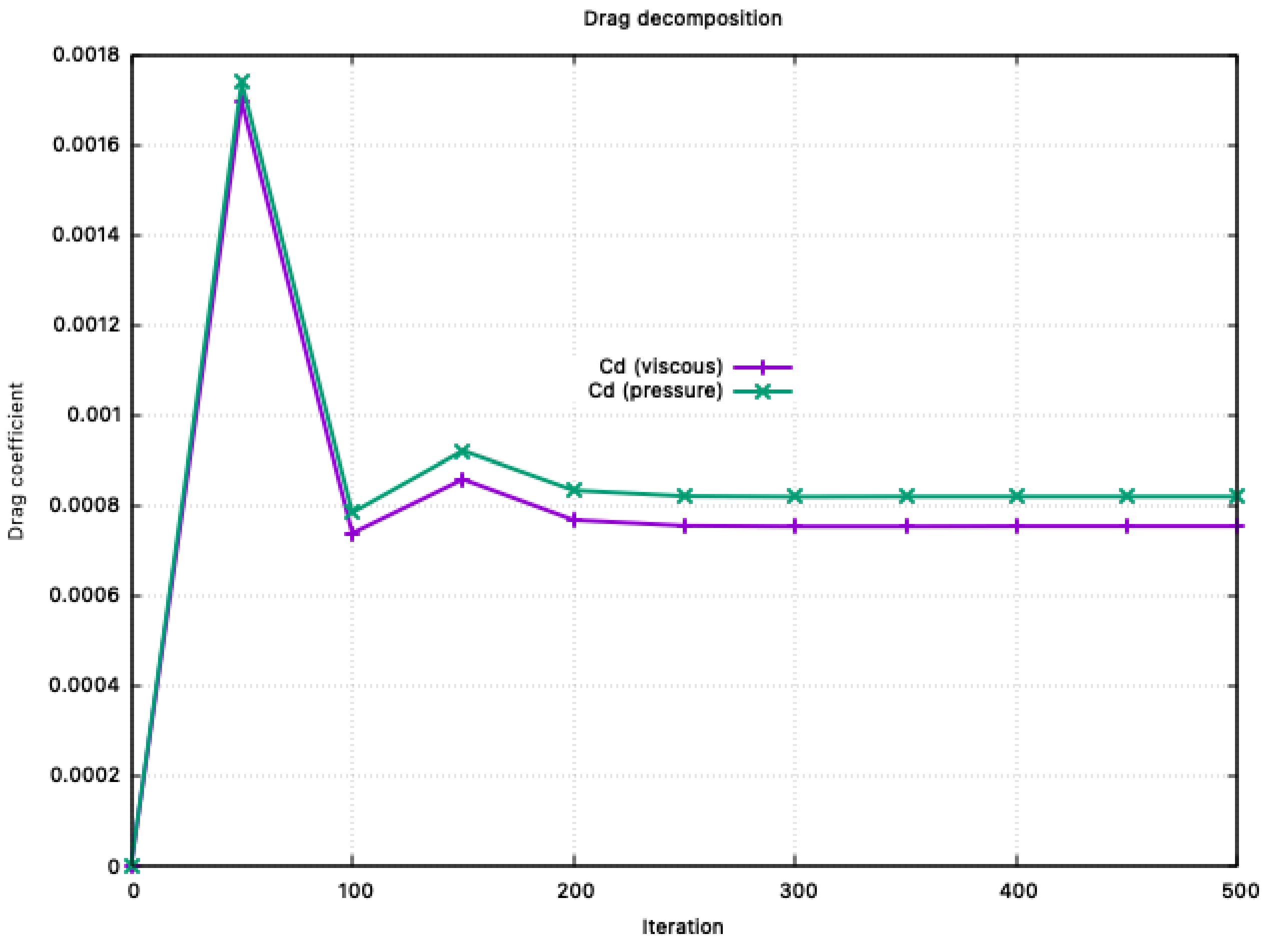

Lift decomposition vs iterations

Lift decomposition splits the lift into pressure and viscous contributions. Here, the viscous (shear) term is the dominant part of the lift, while the pressure contribution is smaller. Both components level off after ~200 iterations, indicating the force solution is converging.

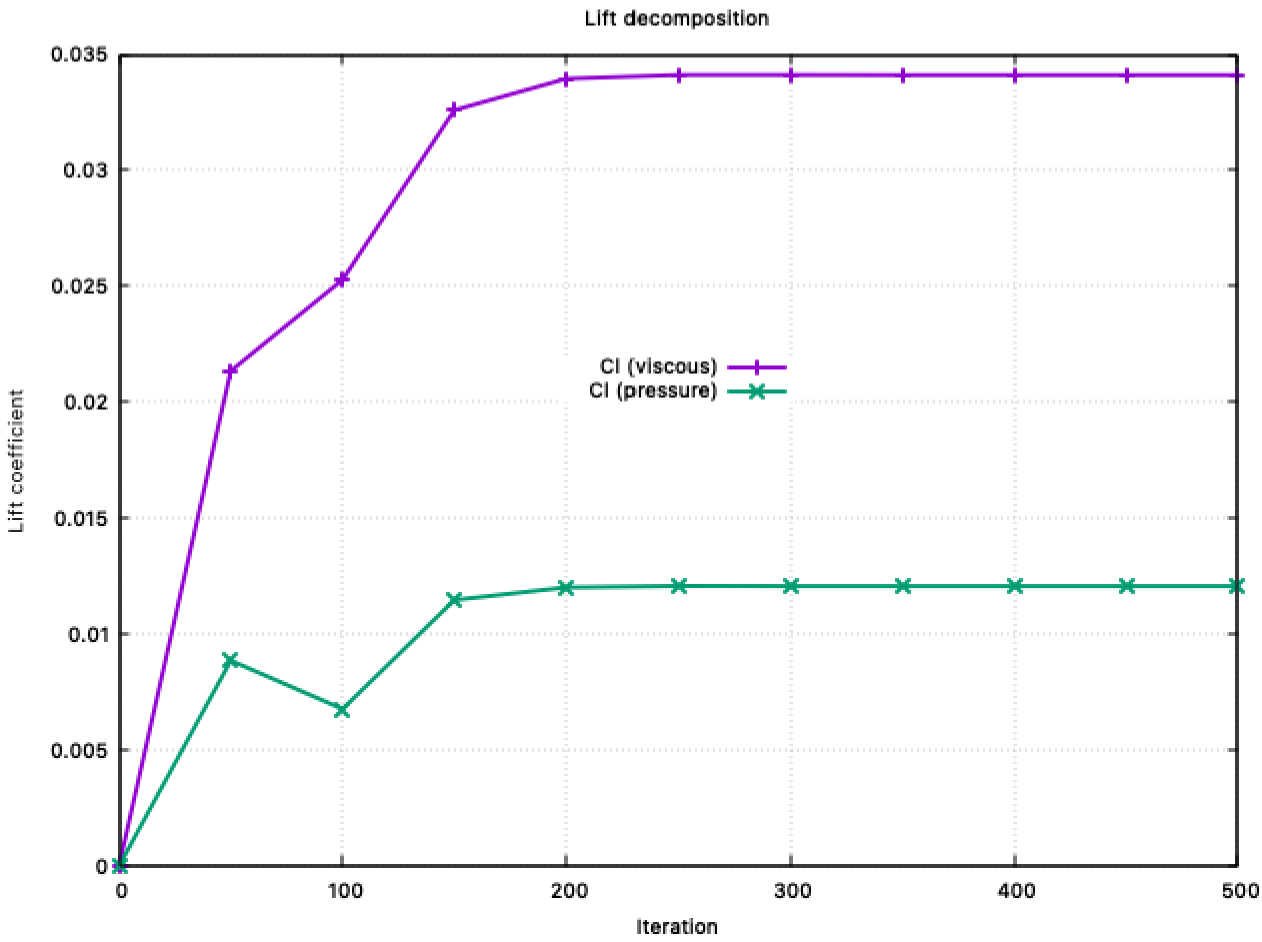

Pitching moment coefficient vs iterations

The pitching moment coefficient C_m converging indicates the aerodynamic loading distribution has stabilised and the steady solution is consistent.

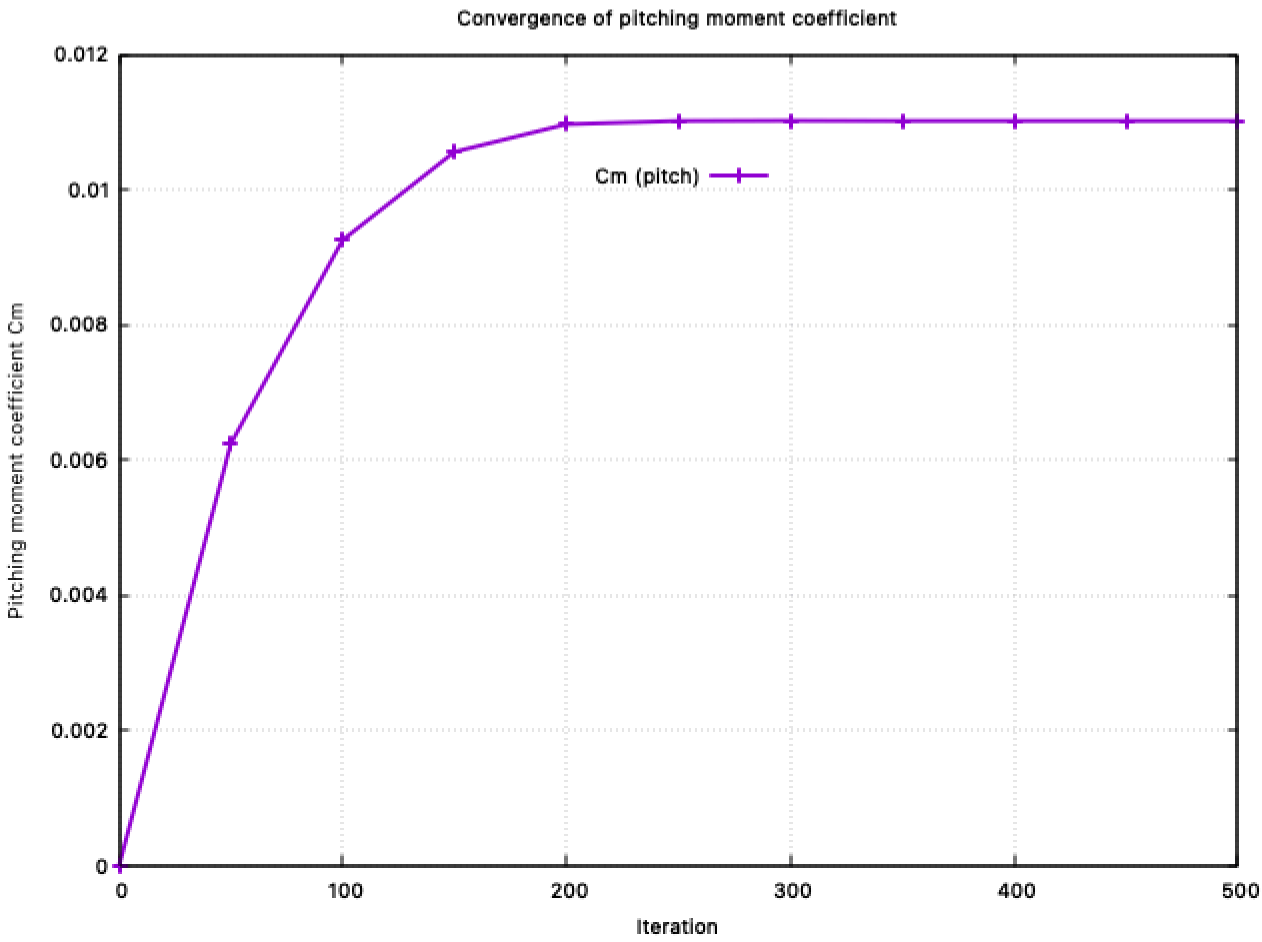

Pressure coefficient as a function of normalized chord length

This plot shows how the pressure coefficient varies along the airfoil chord on the suction and pressure sides. A strong suction peak (more negative Cp) typically appears near the leading edge on the suction side, and Cp gradually recovers toward the trailing edge. The pressure-side Cp is usually higher (less negative / more positive), and the difference between the two curves represents the pressure-driven contribution to lift.

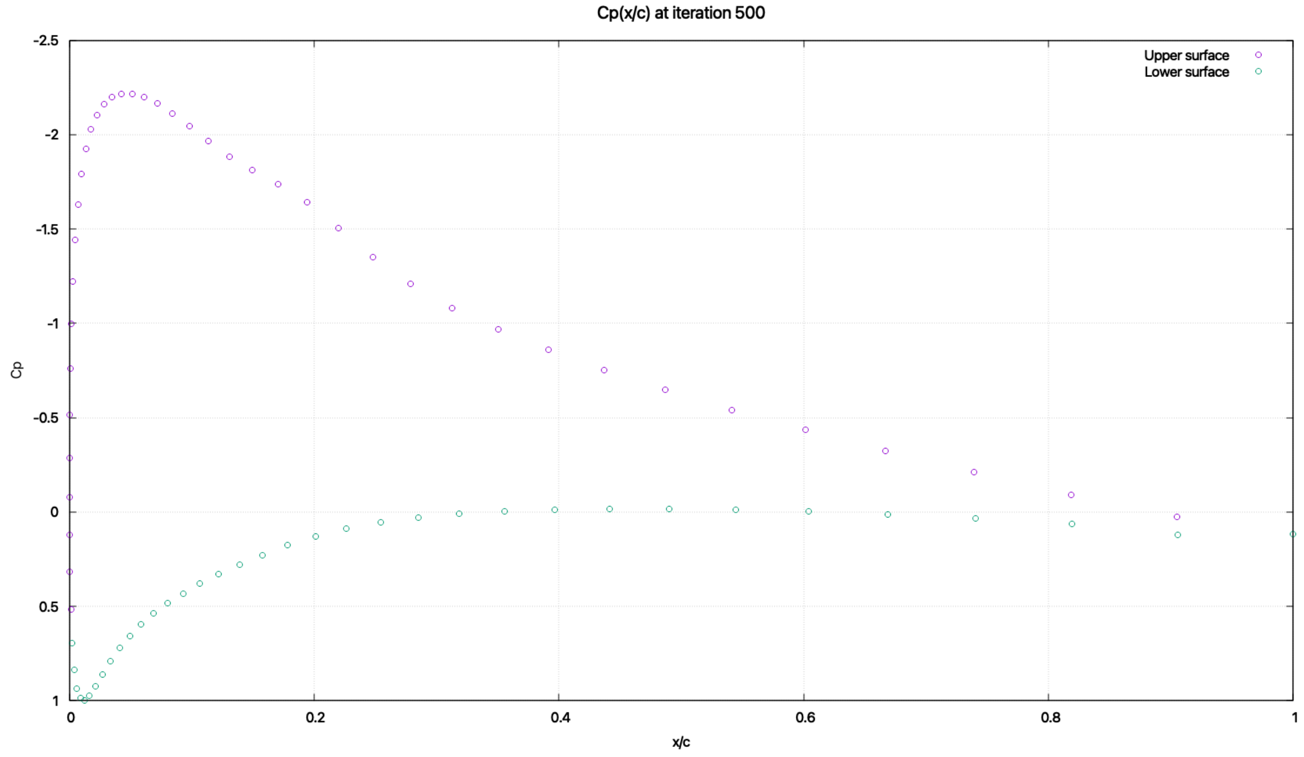

2D cylinder

This case is laminar flow past a 2D cylinder for multiple Reynolds numbers $(Re = 100, 400, 1000, 4000)$ using `pimpleFoam`. The cylinder has $D = 1$ m and the free stream velocity is $U = 1$ m/s.

The block layout illustrates a structured mesh strategy that contains 20 blocks: finer blocks near the cylinder and in the wake to capture boundary layers and vortex shedding.

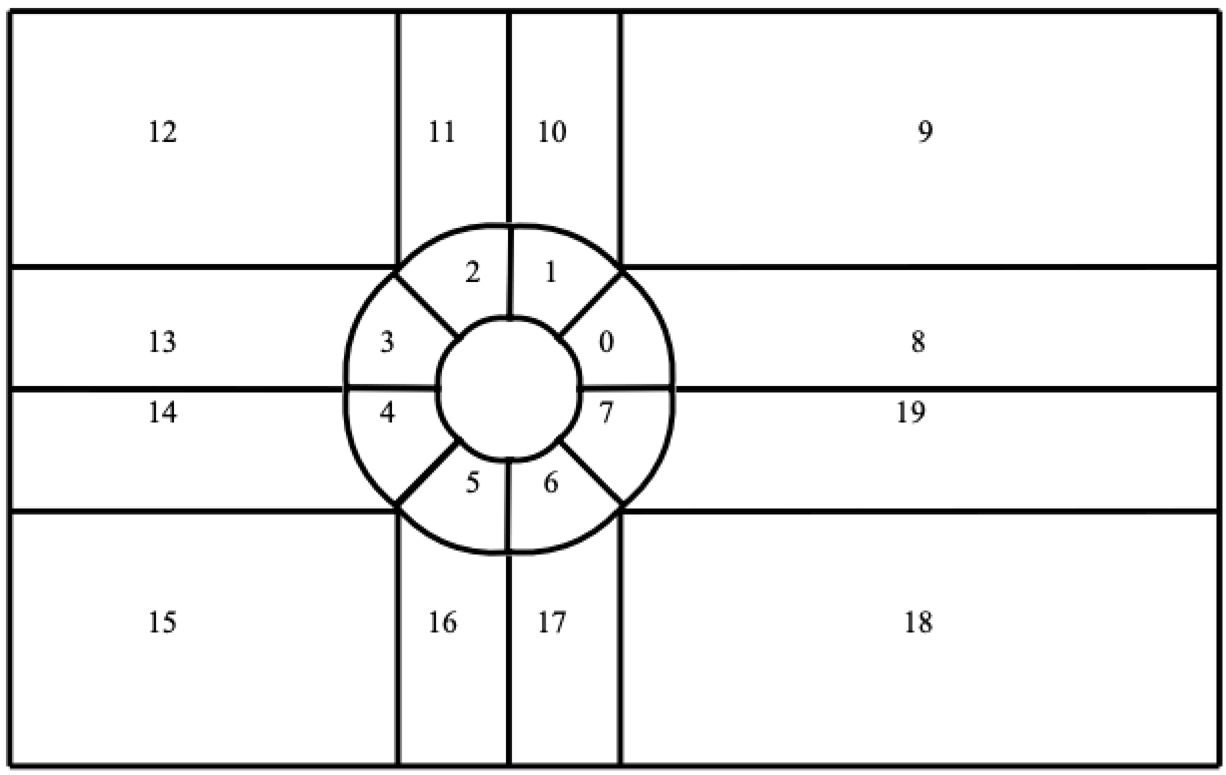

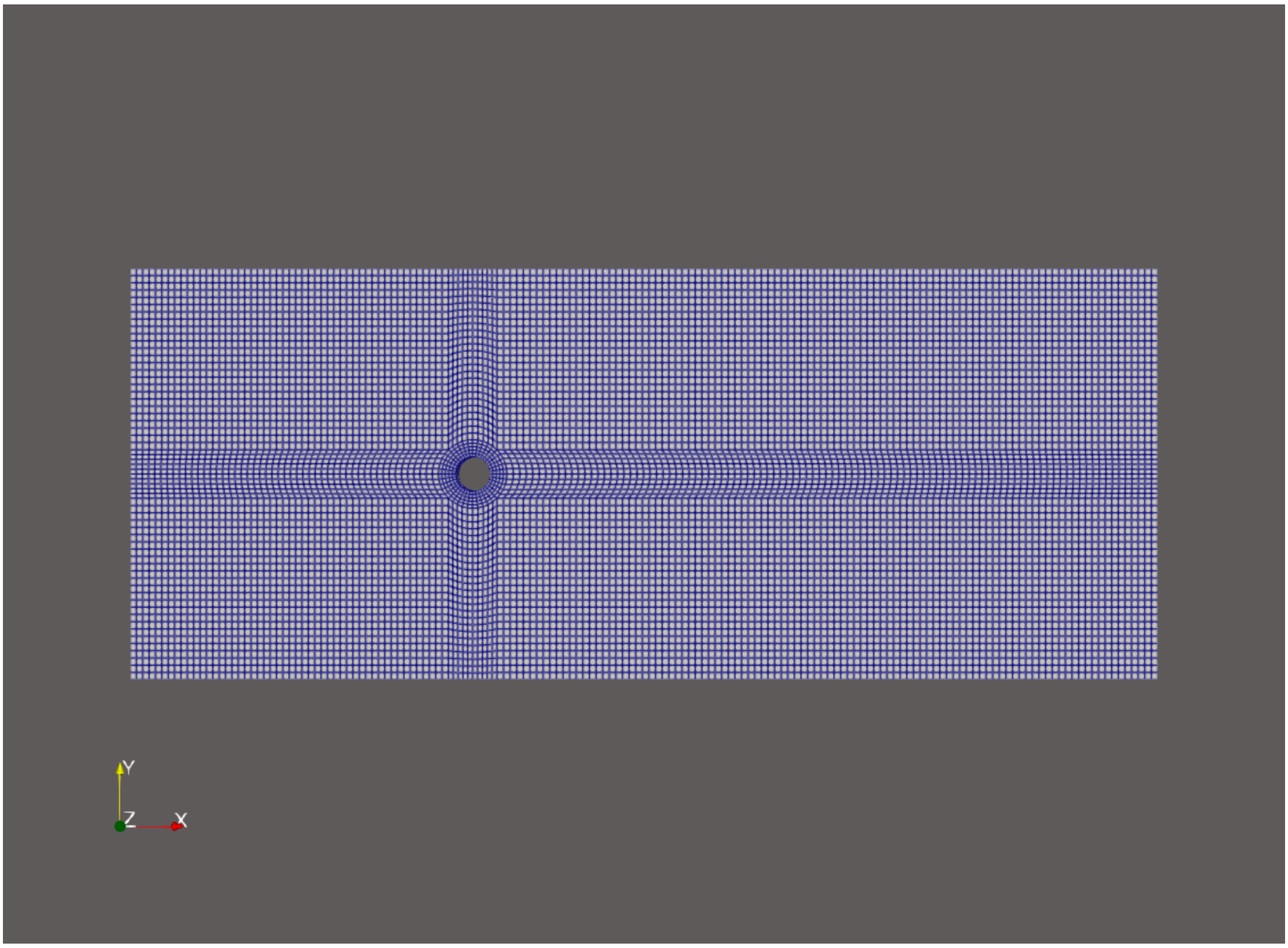

Velocity contours

The velocity magnitude plot shows a wake region downstream with reduced velocity (velocity deficit) and stronger gradients around the cylinder surface, which are key drivers of drag and unsteady wake dynamics.

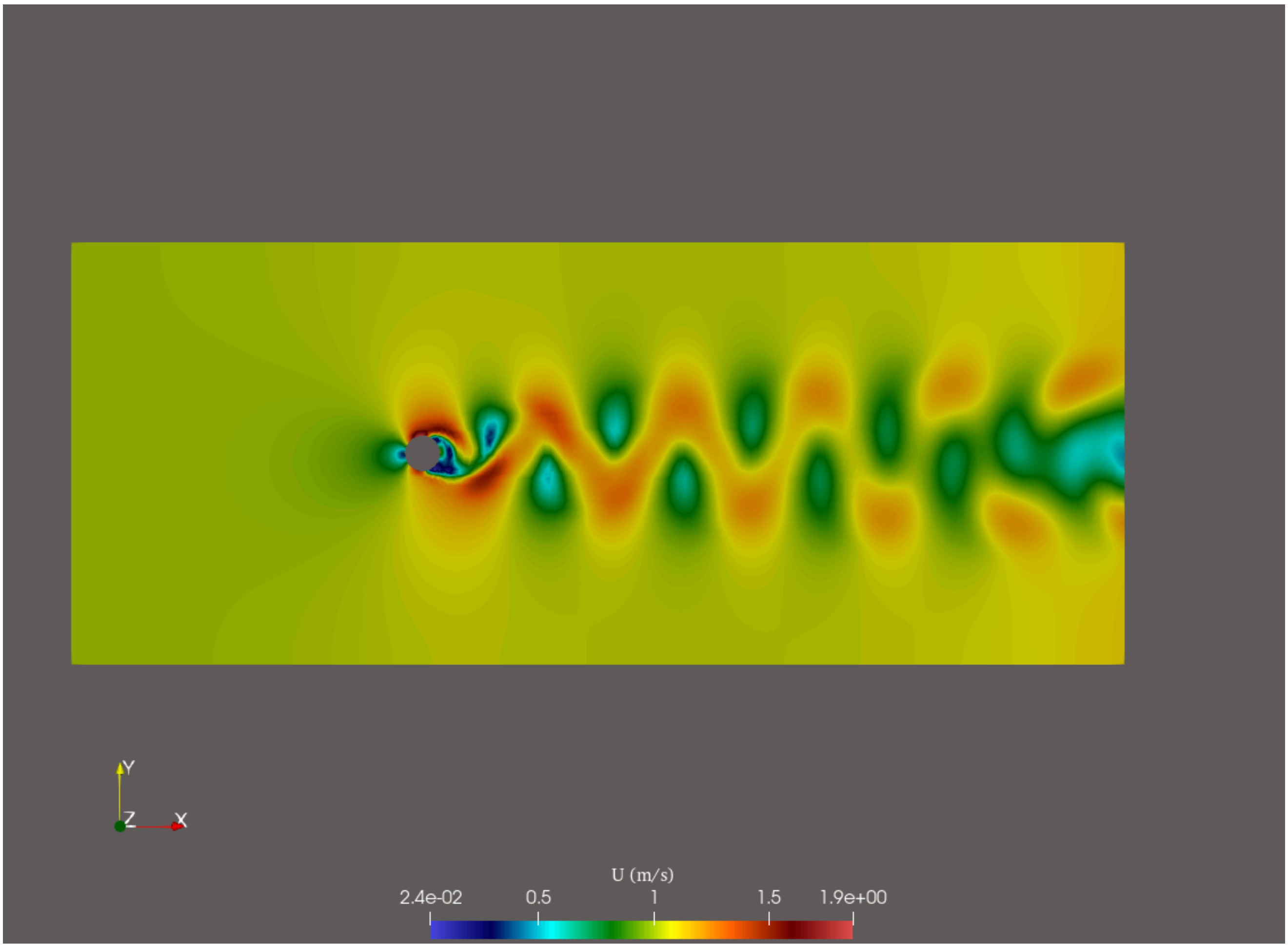

Streamfunction

The streamfunction shows alternating swirling structures in the wake—this is the von Kármán vortex street that forms when vortex shedding develops.

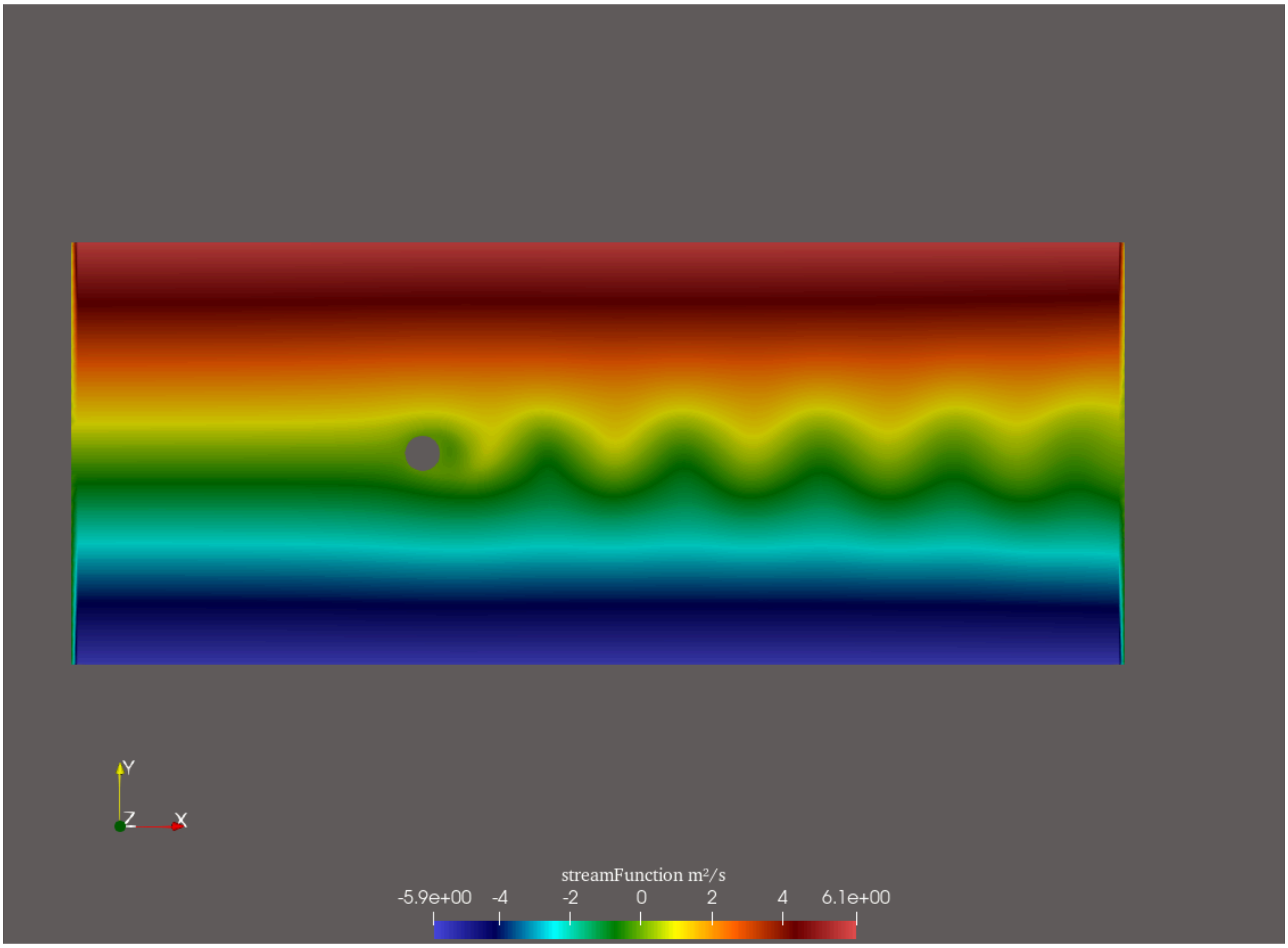

Vorticity magnitude

The vorticity magnitude highlights where rotation is strongest and makes the shedding pattern more visible. The snapshot illustrates the alternating wake pattern responsible for unsteady forces.

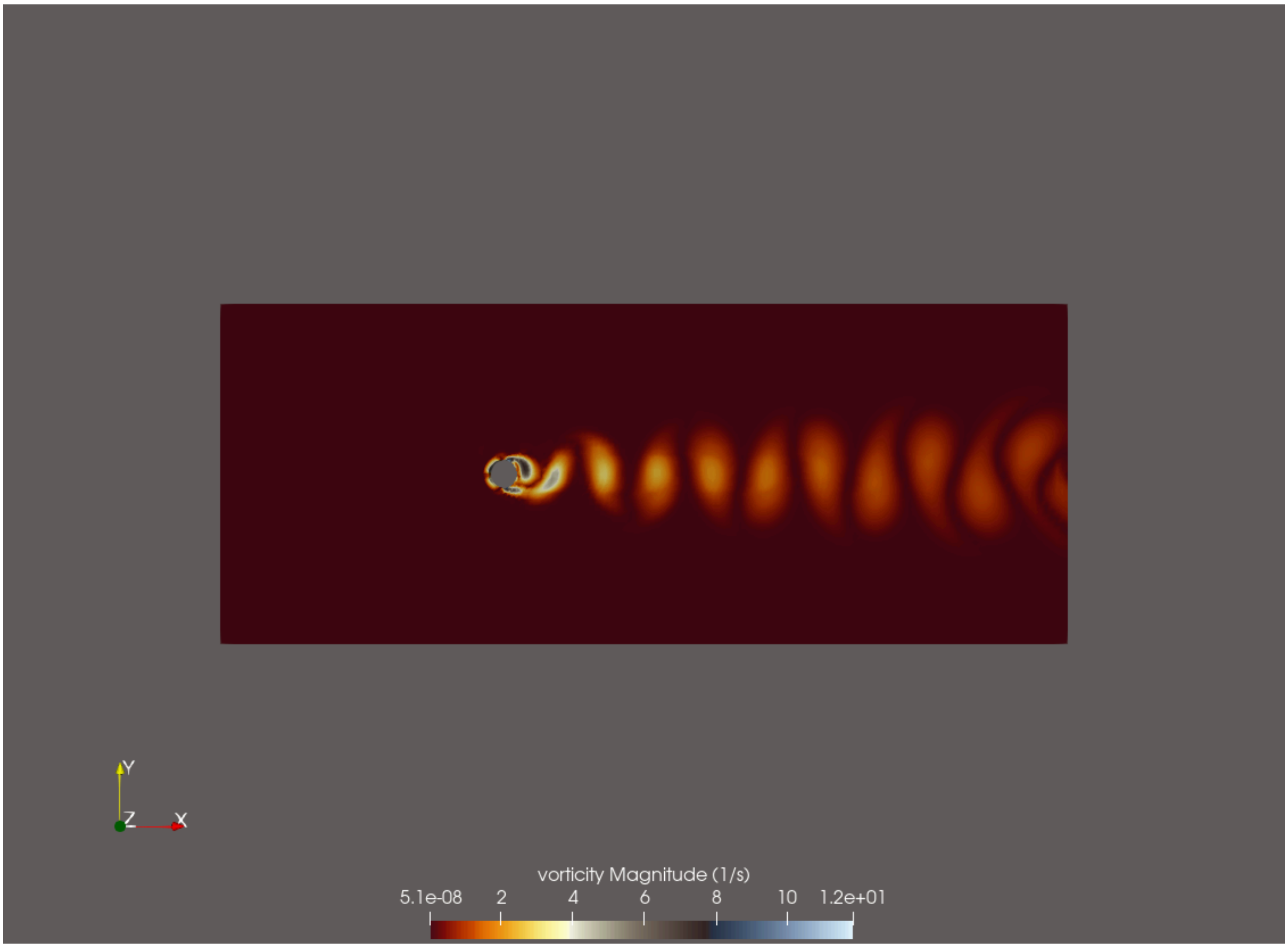

Lift coefficient vs time

The lift coefficient C_l oscillates because vortices are shed alternately from each side of the cylinder. Typically, increasing Re leads to stronger and more regular shedding, which changes both amplitude and frequency of $C_l(t)$.

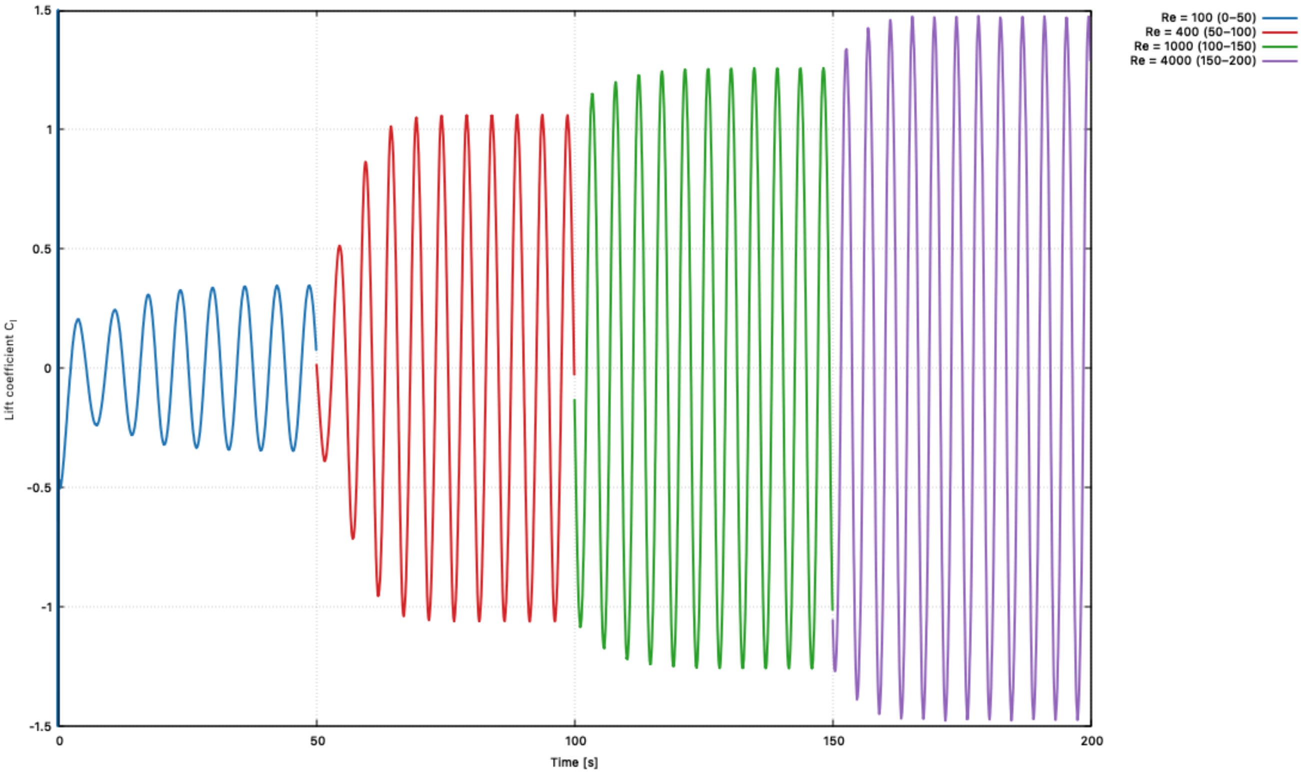

Drag coefficient vs time

The drag coefficient $C_d(t)$ also becomes periodic once shedding is established (often with a different waveform than lift).

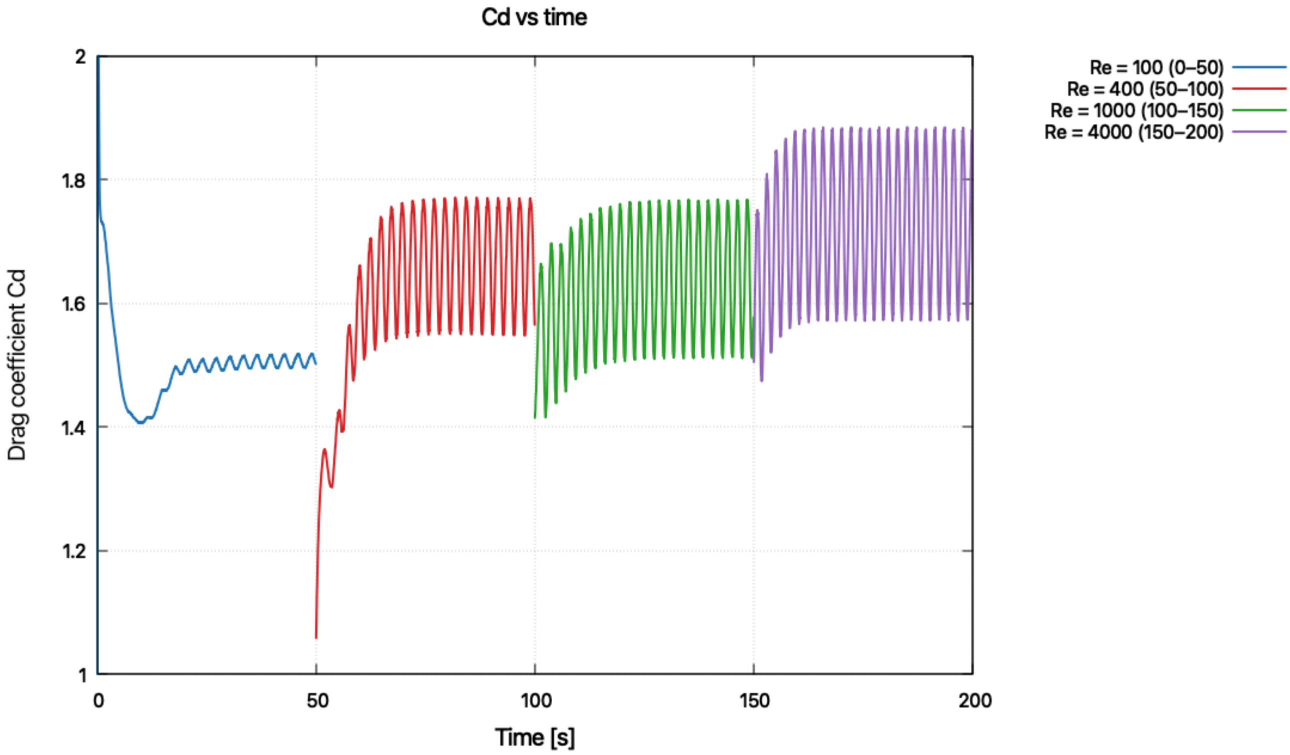

Strouhal number vs Reynolds number

The Strouhal number plot summarizes shedding frequency versus Reynolds number (extracted from $C_l(t)$), showing how vortex shedding frequency changes with Re and tends to level off in a certain range for higher Re.

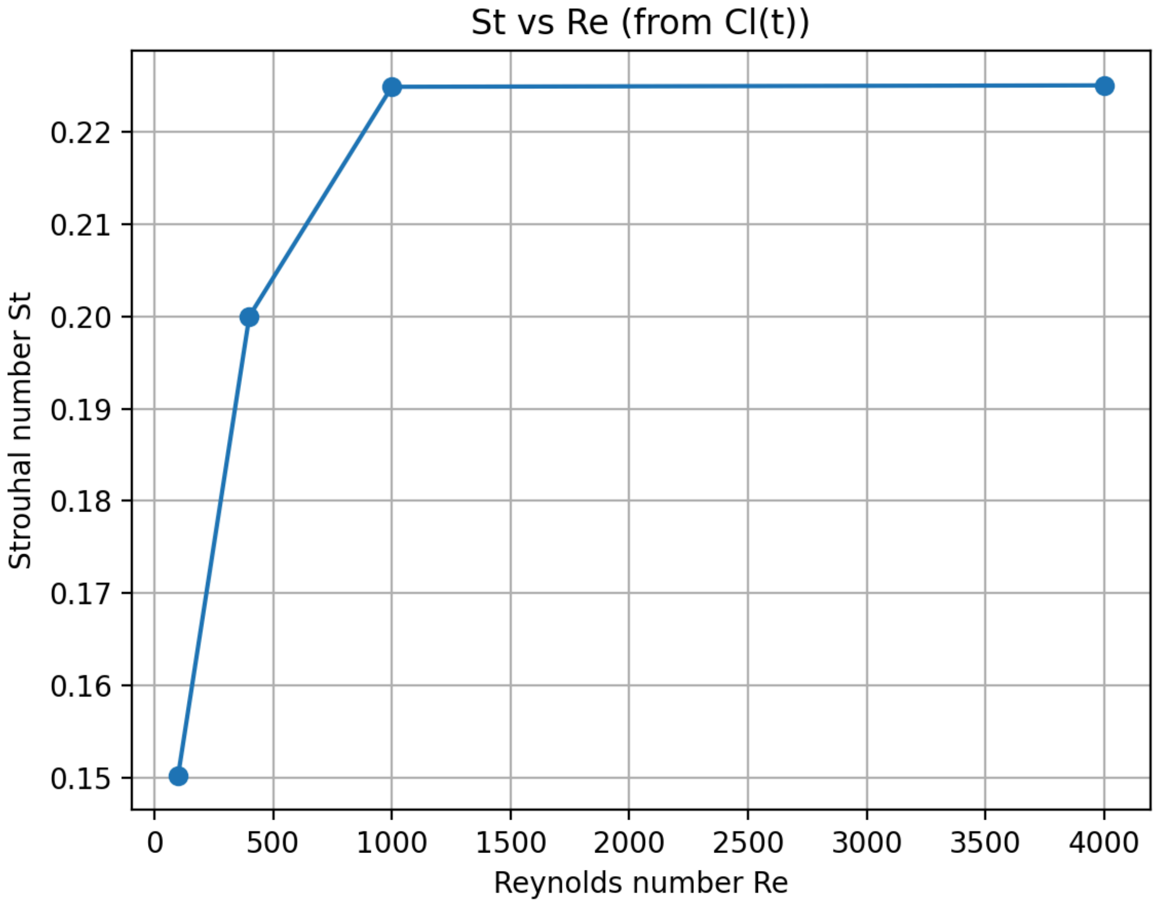
St vs Re (from Cl(t))
Strouhal number St
0.22
0.21
0.20
0.19
0.18
0.17
0.16
0.15
0
500
1000
1500
2000
2500
3000
3500
4000
Reynolds number Re